Biofilm-associated *Mycobacterium abscessus* cells have altered antibiotic tolerance and surface glycolipids in Artificial Cystic Fibrosis Sputum Media.

Augusto Cesar Hunt-Serracin[1], Brian J. Parks[1], Joseph Boll[1] and Cara Boutte[1*]

[1]Department of Biology, University of Texas Arlington

[*]Corresponding author: cara.boutte@uta.edu

Abstract

Mycobacterium abscessus (*Mab*) is a biofilm-forming, multi-drug resistant, non-tuberculous mycobacterial (NTM) pathogen increasingly found in Cystic Fibrosis patients. Antibiotic treatment for these infections is often unsuccessful, partly due to *Mab*'s high intrinsic antibiotic resistance. It is not clear whether antibiotic tolerance caused by biofilm formation also contributes to poor treatment outcomes. We studied the surface glycolipids and antibiotic tolerance of *Mab* biofilms grown in Artificial Cystic Fibrosis Sputum (ACFS) media in order to determine how they are affected by nutrient conditions that mimic infection. We found that *Mab* displays more of the virulence lipid trehalose dimycolate when grown in ACFS compared to standard lab media. In ACFS media, biofilm-associated cells are more antibiotic tolerant than planktonic cells in the same well. This contrasts with standard lab medias, where biofilm and planktonic cells are both highly antibiotic tolerant. These results indicate that *Mab* cell physiology in biofilms depends on environmental factors, and that nutrient conditions found within Cystic Fibrosis infections could contribute to both increased virulence and antibiotic tolerance.

24 **Introduction**

25 Infections caused by Non-Tuberculous Mycobacteria (NTM) are on the rise across the
26 globe (1-3). *Mycobacterium abscessus* (*Mab*) is a highly antibiotic-resistant NTM that
27 causes soft tissue infections and is an increasingly common respiratory pathogen in
28 Cystic Fibrosis (CF) patients (4-6). While most NTM infections are believed to be
29 contracted through environmental exposure, *Mab* has recently been shown to be
30 transmitted between CF patients, probably by fomites (7). Unfortunately, *Mab* infections
31 in CF patients are very difficult to treat, and there are no standardized treatment
32 regimens. Treatment usually involves some combination of clarithromycin, amikacin,
33 imipenem, cefoxitin and/ or linezolid(8). Infection clearance after up to 3 years of
34 antibiotic treatment is achieved in only 10-55% of patients (8). This level of treatment
35 failure is likely partly due to intrinsic antibiotic resistance (9-11); however, antibiotic
36 tolerance may also play a role (12), though the environmental conditions that induce
37 tolerance in this organism are poorly understood.

38

39 The pathophysiology of *Mab* infection in the CF lung has scarcely been studied, but one
40 pathology study of explanted lungs from CF patients showed *Mab* aggregates that
41 appear to be forming a biofilm around the alveoli (13). Biofilms are bacterial
42 communities that in many species are held together by exopolysaccharides (14).
43 Mycobacterial biofilms appear to depend on surface glycolipids (15) and free mycolic
44 acids (16, 17), though many questions remain about the composition of the matrix in
45 mycobacterial biofilms. Because bacteria growing in biofilms are notoriously tolerant to
46 antibiotics (18), this mode of growth during infection may contribute to the treatment

47 recalcitrance of *Mab*. While we currently lack a comprehensive model of the chemical
48 and genetic basis of *Mab* biofilm formation, it is clear that surface glycolipids are
49 important. Glycopeptidolipids, which are found on the outer leaflet of the mycobacterial
50 outer membrane, have been shown to affect biofilm structure (19) and are thought to
51 modulate the course of infection (20, 21). Trehalose dimycolate (TDM), which is known
52 to contribute to virulence in *Mtb* (22) are also found on the surface of some *Mab* strains,
53 though its contribution to biofilm formation and virulence in *Mab* has not been studied.
54
55 *Mab* has two genetic isoforms: the wild-type “smooth” strains, which produce abundant
56 GPLs and minimal TDM, and “rough” mutants, which have genetic lesions in the GPL
57 loci and display little or no GPLs but sometimes have higher levels of TDM (23, 24). The
58 smooth strains form more robust biofilms and it is thought that this form could contribute
59 to colonization at infection sites (24), which is likely promoted by GPLs masking other
60 cell surface molecules that activate innate immunity (21). The rough mutants cause
61 more inflammation (21), are more virulent, and are thought to promote more tissue
62 invasion (24). Rough mutants are more frequently isolated after a persistent infection
63 has been established for a long period, in both CF and non-CF patients (25, 26).
64
65 The smooth and rough genetic variants represent two phenotypic extremes of *Mab*
66 physiology. However, the rough variants only form in some infections, and it is thought
67 that most infections are established by smooth strains (24). Smooth strains are known
68 to form biofilms *in vitro* (12, 19) and are thought to also form biofilms during infection
69 (13). Antibiotic-recalcitrant *Mab* infections are likely to involve mature biofilms growing in

complex nutrient environments. However, *in vitro Mab* biofilm studies have been done on immature biofilms in simple nutrient environments (12, 19): in these conditions there are modest differences in antibiotic tolerance between biofilm-associated and planktonic cells (19). Thus, it is not clear to what extent biofilms contribute to antibiotic tolerance during infection.

In this work, we sought to determine how cell surface physiology, biofilm formation and antibiotic tolerance are affected by media conditions in *Mab* ATCC19977. We find that the cell surface, as measured by fluorescent staining, is different in *Mab* in Artificial Cystic Fibrosis Sputum (ACFS) media compared to either minimal HdB media or in the standard mycobacterial growth media, 7H9. In addition, both smooth and rough strains display more TDM in the ACFS media. When we compare biofilm and planktonic cells, we find that both populations are quite antibiotic tolerant in HdB and 7H9, while the planktonic cells are more susceptible to antibiotics in ACFS media.

Results

To determine how different nutrient conditions affect basic cell physiology, we measured growth rate and microscopically examined *Mab* in three different media. *Mab* grows fastest in 7H9 media (Fig 1AB), even though the Artificial Cystic Fibrosis Sputum (ACFS) media is richer (27). *Mab* in ACFS media appears to die off more in stationary phase, implying that the nutrient richness may not prepare cells for certain stresses (Fig. 1A). We imaged cells using phase microscopy and observed that cell lengths were longer in ACFS media (Fig. 1CD). We stained log. phase cells in each media with both

93 NADA, a 4-chloro-7-nitrobenzofurazan-conjugated D-alanine (28), which is integrated
94 into peptidoglycan, and FM4-64, which stains the inner membrane (29). Although
95 growth rates were more similar in HdB and ACFS media, cell surface staining was more
96 similar in HdB and 7H9. The NADA staining in Hdb and 7H9 was consistent with studies
97 performed in other mycobacterial cells: brighter staining at the septa and poles where
98 new peptidoglycan is inserted (30). FM4-64 stained most cells in these media types
99 dimly, but a subset stained more brightly. Staining of cells in ACFS media was more
100 homogeneous (Fig. 1DE). We observed in the phase images that cells growing in ACFS
101 appear to be encased in translucent sheaths, which could alter access of the stains to
102 the cell (Fig. 1D). These data show that *Mab* is physiologically different in typical lab
103 media than in media that mimics the nutrient conditions in the lungs of Cystic Fibrosis
104 patients.
105
106 In order to study the physiology of biofilms, we sought to develop a method to separate
107 biofilm and planktonic cells from the same culture well: this allows us to control
108 internally for nutrient depletion in the media, which also impacts cell physiology and
109 antibiotic tolerance. We incubated standing cultures in tissue culture-treated plates.
110 Biofilms form at the bottom of each well, while the planktonic cells remained in the
111 media in the upper half of the well. We pipetted off all the media on the top of each well
112 to isolate planktonic cells, then resuspended the surface-associated cells on the bottom
113 of each well in 7H9 with Tween80, a non-ionic detergent, which broke apart cell clumps.
114 To determine whether 7H9 + Tween80 was sufficient to break apart clumps or whether
115 sonication was necessary, we compared the colony forming units (CFU) produced from

116 biofilm resuspensions with and without sonication (Fig. S1). Sonication did not change
117 the CFU counts, so we conclude that resuspension in 7H9 + Tween80 alone is sufficient
118 to break apart smooth *Mab* biofilms. Therefore, we used that method for biofilm
119 enumeration in subsequent experiments.
120
121 We next analyzed how the three media types affect biofilm development and
122 morphology. We grew *Mab* in the three different media types over time and monitored
123 biofilm development by CFU assay and photography. Biofilms growing in all media
124 types reach maximal cell density by day 6 (Fig. 2). Biofilms in ACFS form three-
125 dimensional plumes in standing culture, while those in HdB or 7H9 are flat and almost
126 crystalline. We did not observe pellicles in the media conditions we tested using smooth
127 *Mab* strains (Fig. 2). From these data we conclude that biofilm morphology was affected
128 by media condition.
129
130 To probe the physiological differences between biofilm and planktonic cells in our
131 assay, we tested their ability to transcriptionally and translationally respond to induction
132 of a reporter. We transformed *Mab* with a plasmid that expresses Tag-RFP under the
133 control of a constitutive P_{GroEL} promoter, and expresses eGFP under control of an
134 inducible $P_{nitrile}$ promoter. We allowed biofilms of this culture to mature for 6 days, then
135 induced them with isovaleronitrile to induce expression of eGFP. After 24 hours of
136 induction, we resuspended and fixed cells from the planktonic and biofilm populations in
137 each media type, and visualized the cells by fluorescence microscopy (Fig. 3A). We
138 found that in all media conditions, cells in biofilms are less likely than planktonic cells to

139 express significant eGFP upon induction, compared to the constitutive Tag-RFP (Fig.
140 3B). This shows that biofilm cells are either less permeable to the inducer, or are less
141 transcriptionally and translationally active than planktonic cells in the same culture well,
142 or both. These data also validate our method of separating planktonic cells from biofilm
143 cells, by showing separated cell types are physiologically distinct in all three media
144 types.
145
146 Because biofilm morphology varied so greatly between media types (Fig. 2), we
147 hypothesized that media could affect glycolipid expression. We extracted surface
148 glycolipids from planktonic smooth and rough strains grown in 7H9 and ACFS (Fig. 4A)
149 as well as from mature biofilms grown in all three media conditions (Fig. 4B). We then
150 separated the glycolipids by thin layer chromatography (TLC). TLC analysis shows that
151 the smooth strain expresses similar levels and types of GPLs irrespective of media
152 condition, while the rough strain produces minimal GPLs (Fig. 4A). In biofilms, the
153 smooth strain expresses GPLs in all conditions (Fig. 4B,D). Based on previous GPL
154 analyses (24), the purple spot near the top (Fig. 4B, spot c) is an unidentified wax, while
155 the dark purple spot at the bottom (Fig. 4B, spot d) is trehalose dimycolate (TDM) (31).
156 Both smooth and rough strains have increased TDM in ACFS compared to lab media, in
157 both planktonic cultures (Fig. 4A) and biofilms (Fig. 4B). We observe a statistically
158 significant increase in the wax (Fig. 4B,C) and TDM in ACFS (Fig. 4B,E). The levels of
159 GPLs appear to be similar (Fig. 4B, D). These data show that media conditions affect
160 the surface glycolipid expression of *Mab* and that *Mab* grown in ACFS media has higher
161 levels TDM, a glycolipid that is a virulence factor in *Mtb* infections (22).

162

163 We sought to determine how biofilm maturity affects antibiotic tolerance. For these and
164 all subsequent biofilm experiments, we compared survival of biofilm and planktonic cells
165 from the same well of a 24-well plate for each replicate. We incubated *Mab* in ACFS
166 media for 3, 6 or 11 days, then treated each well with two clinical drugs, clarithromycin
167 and imipenem. We then measured survival over time and found that tolerance increases
168 over time in standing culture, likely due to nutrient depletion of the media (Fig. 5AB). In
169 3-day and 6-day old biofilms, planktonic cells die off substantially upon treatment, while
170 at 11 days both populations are quite tolerant (Fig 5A). 6-day old biofilms had higher
171 tolerance compared to the planktonic cells in the same well at both 24 and 48 hours of
172 treatment (Fig. 5B). From this, we conclude that at six days the biofilms in ACFS media
173 are mature enough to substantially protect cells against antibiotics. Based on these
174 results, and the fact that biofilms in all media types reached maximal cell density at six
175 days (Fig. 2), we conducted all subsequent biofilm assays with 6-day old biofilms.
176

177 In order to determine how media type affects the antibiotic tolerance of *Mab* biofilms, we
178 treated 6-day old biofilms grown in different media types with varying concentrations of
179 the clinically used antibiotics amikacin, clarithromycin and cefoxitin, and then plated
180 both the biofilm and planktonic cells at 48 hours after treatment. We found that amikacin
181 consistently killed planktonic cells at nearly an order of magnitude more than the biofilm
182 cells from the same well, across media types. With clarithromycin and cefoxitin
183 treatment, however, we saw much more variability. With both these antibiotics,
184 planktonic cells and biofilm-associated cells were both highly antibiotic tolerant in both

185 7H9 and HdB. However, in ACFS, planktonic cells were much more sensitive to
186 clarithromycin and cefoxitin than biofilm-associated cells. Clarithromycin was the only
187 drug that was able to kill biofilm-associated cells at concentrations below 50 µg/ml, and
188 this only occurred in ACFS media (Fig. 6).
189
190 In our assays, the biofilm-associated cells are likely to have access to less oxygen than
191 the planktonic cells. We sought to determine whether hypoxia could differentially affect
192 cells depending on the media. We made cultures of *Mab* in tubes with minimal
193 headspace, sealed the tubes with septum caps, and incubated them without shaking for
194 13 days. We then injected cefoxitin through the caps and measured survival after 48
195 hours. Results show that hypoxic *Mab* exhibits tolerance in both 7H9 or ACFS media
196 (Fig. S2), comparable to that seen in biofilms (Fig.6AB). Thus, as for *Mtb* (32), hypoxia
197 promotes antibiotic tolerance in *Mab* and is likely to be one factor in the antibiotic
198 tolerance seen in biofilm-associated cells.
199
200 **Discussion**
201 Bacterial physiology is enormously plastic. Bacterial cell size, shape, growth rates,
202 surface properties and gene expression all change profoundly even between different
203 lab media conditions (33-35). This plasticity makes it very difficult to determine the
204 physiological state of a pathogen during infection. In this study, we sought to
205 physiologically profile the emerging pathogen *M. abscessus* in two standard lab growth
206 medias and one media designed to mimic the nutrient conditions in the lungs of Cystic
207 Fibrosis patients (ACFS). We find that, compared to standard lab medias, ACFS media

208 induces profound physiological changes in *Mab*, both in planktonic (Fig.1, Fig. 4) and
209 biofilm states (Fig.4, Fig.6).
210
211 Bacterial biofilms are complex structures which, on the macro scale, vary physiologically
212 according to developmental stage (36), surface type (37) and nutrient conditions (38).
213 On the microscopic scale, there is also heterogeneity within a single biofilm: cells in
214 different places within the biofilm express different surface factors and have different
215 gene expression profiles (39-41). Thus, it is not meaningful to merely compare the
216 phenotypes of “biofilm” and “planktonic” cells from a given species, as there is
217 enormous phenotypic variety within each of these categories. In this work, we profiled
218 some of the phenotypic diversity possible in *Mab* biofilms in order to assess the extent
219 to which *in vitro* biofilm experiments might be relevant to the physiology of *Mab* biofilms
220 within the lungs of CF patients. Our results show that *Mab* biofilms in ACFS media have
221 important physiological differences from biofilms in the standard mycobacterial lab
222 medias HdB and 7H9 (Fig. 2, Fig.4, Fig.6). The fact that such differences can be seen
223 even between *in vitro* media conditions shows that *Mab* biofilm physiology is responsive
224 to environmental conditions. We hypothesize that *Mab* physiology in HdB and 7H9
225 media is unlikely to represent its physiology during infection. Our results do not
226 establish ACFS media as a proxy for infection, which of course includes many host
227 immune factors that cannot be mimicked *in vitro*. However, these data show that
228 nutrient conditions that might be encountered by *Mab* in the host could have an
229 important role in the pathogen’s expression of virulence glycolipids and responsiveness
230 to antibiotic treatment.

231

232 Even in experiments with the smooth *Mab*, which produces GPLs, we observed
233 differences in the appearance of the biofilms that formed in the different media types.
234 The biofilms in both HdB and 7H9 appeared flat and flaky, while the biofilms that formed
235 in the ACFS media looked wet and formed tendrilly plumes (Fig. 2). These differences
236 could be merely due to the chemical and viscosity differences between the media types,
237 or they could be due to changes in *Mab* cell physiology in the different media types. We
238 profiled the surface glycolipids and antibiotic sensitivity of cells in these different
239 biofilms, and found that cells in ACFS biofilms are physiologically distinct: they display
240 more trehalose dimycolate and a non-polar wax species than biofilms in 7H9 and HdB
241 (Fig. 4) and they exhibit more relative antibiotic tolerance compared to planktonic cells
242 (Fig. 6).

243

244 Because nutrient availability affects the physiology of cells within a biofilm, we sought to
245 develop methods that would allow us to disentangle responses to nutrients from
246 responses to biofilm formation. Other groups solved this problem by moving biofilms to
247 fresh media each day (12, 19). We assumed that nutrients would not be unlimited
248 during infection, and so worked to assess biofilm physiology in nutrient-limited culture
249 (Fig. 2, Fig. 5). In order to control for the well-known effects of nutrient limitation on
250 antibiotic tolerance (42), we compared biofilm and planktonic cells from the same
251 culture wells. These cells are sharing the same depleted nutrients, so differences in
252 physiology should be due to association with the biofilm, or to differences in access to
253 oxygen. While we observed considerable antibiotic tolerance in 7H9 and HdB against

254 clarithromycin and cefoxitin, there was similar tolerance in planktonic and biofilm-
255 associated cells (Fig. 6B,C), even though the planktonic cells presumably have more
256 access to oxygen at the top of the well. This implies that antibiotic tolerance in these
257 media conditions is due to some other environmental factor, such as nutrient depletion,
258 rather than due to the protection of the biofilm or to hypoxia. In the more nutrient-rich
259 ACFS media however, we see much higher sensitivity to cefoxitin and clarithromycin in
260 the planktonic cells, while the biofilm-associated cells are tolerant. Therefore, the
261 physiological difference between biofilm and planktonic cells is greater in ACFS media
262 than in typical lab medias.
263
264 Our results imply that the modest degree of antibiotic tolerance in biofilms that has been
265 observed before (19) may be a function of the culture conditions. Our data show that
266 mature biofilms grown in ACFS media afford considerable protection against three
267 clinical antibiotics from different classes. While the ACFS media may mimic the nutrient
268 conditions of sputum, it does not replicate a complex host environment with active
269 immune cells and tissue structures, so the physiological state of *Mab* in a true infection
270 remains unknown. However, our results imply, during infection in CF patients, *Mab* may
271 express more of the virulence glycolipid TDM, and be more antibiotic tolerance that
272 experiments in regular lab media might indicate. Thus, treatments that could help
273 disrupt *Mab* biofilms or prevent their establishment could help clear these infections
274 more quickly. A deeper understanding of the chemistry and genetics of biofilm formation
275 and physiological responses in *M. abscessus* will be needed in order to determine the

276 role of biofilms in infection and treatment recalcitrance and to develop better treatment
277 protocols.
278
279 **Materials and Methods**
280 *Media and culture conditions.* All *M. abscessus* ATCC19977 cultures were started in
281 7H9 (Becton-Dickinson, Frankin Lakes, NJ) media with 5 g/l bovine serum albumin, 2g/l
282 dextrose, 0.85 g/l NaCl, 0.003 g/l catalase, 0.2% glycerol and 0.05% Tween80 and
283 shaken overnight at 37C until in log. phase. All *Mab* CFUs were performed by plating
284 serial dilutions on LB Lennox agar. Three media types varying in nutrient richness were
285 used for all biofilm assays: Tween80 was not added to any media for biofilm assay.
286 Hartmans de Bont (HdB) Minimal Media was made as described (43), 7H9 for biofilms
287 was made as above, without the Tween80.
288
289 *Artificial Cystic Fibrosis Sputum.* Two protocols were combined in order to make our
290 ACFS media (27, 44). In 500mL of ultrapure water, the unique components that
291 comprise CF sputum were added as described (44); 5 g of porcine mucin (NBS
292 Biologicals), 4 g of Deoxyribonucleic Acid (Spectrum Chemicals), 5.9 mg diethylene
293 triamine pentaacetic acid (DTPA), 5 g NaCl, 2.2 g KCl, and 1.81 g Tris base. Amino
294 acid stocks were prepared as described (27) and stored at 4C. Except for tryptophan,
295 amino acids were added to the media. The ACFS media was adjusted to a pH of 7,
296 filled-up to one liter, and autoclaved at 110C for 15 minutes. The media was cooled
297 down at room temperature prior to adding tryptophan and 5 mL of egg yolk emulsion
298 (Dalynn Biologicals). ACFS Media was stored at 4C.

299

300 *Biofilm assays.* Log. phase biological replication cultures of *Mab* cultures in 7H9 were
301 inoculated into tissue-culture treated 24-well plates with 2mL of the appropriate media to
302 a final optical density of 0.02. Sufficient wells were inoculated in order to have biological
303 triplicates for each time point or concentration in the assay. Prior to incubation, each
304 plate was covered with a Breathe-Easy sealing membrane (Electron Microscopy
305 Sciences) to allow air exchange and reduce evaporation. Standing biofilm plates were
306 incubated at 37C. The Breathe-Easy membrane was removed after biofilm development
307 in order to add antibiotics. The biofilm plates were then re-sealed and incubated again
308 at 37C for 24 or 48 hours. For each data point, cells from biological replicate wells were
309 used to plate for CFU calculations. To enumerate the planktonic cells, the supernatant
310 was extracted from each well without disturbing the biofilm and plated. The remaining
311 biofilm was then re-suspended in 7H9 + Tween80 and serial dilutions were plated and
312 incubated at 37°C for 4 days. Serial dilutions were done in 96-well plates in HdB +
313 Tween80 and plated on plain LB Agar plates. Relative CFU is the ratio between each
314 CFU value and the initial CFU value at t=0 or concentration=0.

315

316 *Hypoxia Assay. Mab* was grown in 7H9 until log-phase. In order to promote hypoxia,
317 sterile glass tubes were filled near full (9 mL) with 7H9 and ACFS respectively. All tubes
318 were inoculated to an optical density of 0.02, capped with a sterile rubber septum, and
319 wrapped with parafilm to avoid uncapping. To establish growth cessation, standing
320 tubes were incubated at 37C and CFUs were taken every couple days on biological
321 replicates. Once we established that growth cessation happens at 13 days, new tubes

322 were inoculated and incubated for 13 days. In order to avoid oxygenation, replicates
323 were treated by injecting through the rubber septum with 80 μg/mL of cefoxitin. CFUs
324 were taken upon addition of antibiotic (t=0), and 48 hours post-treatment. All time-points
325 were plated on LB Agar and incubated for 4 days.
326
327 *Glycolipid extractions and Thin layer chromatography.* Mature biofilms and planktonic
328 cultures were used for glycolipid extractions. GPLs were extracted as described (34)
329 and spotted on TLC Silica Gel 60 plates (Millipore Sigma). In short, cells were isolated
330 and centrifuged. Pellets were resuspended for lipid extraction in 10mL
331 chloroform/methanol (2:1). Extractions were done twice at room temperature for 24
332 hours and then centrifuged at 5000rpm for 30 minutes to collect organic supernatant.
333 Organic samples (Lipids) were evaporated with nitrogen and resuspended in 1mL
334 chloroform/methanol (2:1) and treated with equal volume 0.2M NaOH (in methanol).
335 Lipids were incubated at 37C for 30 minutes and then neutralized with a few drops of
336 glacial acetic acid. Solvents were evaporated and the lipids were resuspended with 4mL
337 of choloroform, 2mL of methanol, and 1mL of water in each tube. Samples were mixed
338 and then centrifuged at 5000 rpm for 10 minutes to collect the organic layer. The solvent
339 was evaporated and the remaining lipids were resuspended in 100uL of
340 chloroform/methanol (2:1) and spotted. TLCs were developed in chloroform/ methanol/
341 water (100:14:0.8) as described (24). Plates were visualized with 10% Sulfuric Acid (in
342 ethanol) and baked for 20 minutes at 120C. The signal intensity of spots were analyzed
343 and quantified using ImageJ software by means of spot densitometry. For spot d (TDM)
344 the TLC image was split into single color channels and quantified by measuring the

345 signal intensity from the red channel only. Each spot intensity value was normalized
346 against all the spots in a lane (entire lane; all in triplicates). We re-ran the TLCs, when
347 necessary, so that total lane spot intensities were similar between samples.
348
349 *Cell staining.* For experiments on log. phase cells, *Mab* was stained with 3μL/mL of 10
350 mM NADA and incubated at room temperature for 15 minutes in growth media. Cells
351 were then pelleted and resuspended in PBS+Tween80 and FM4-64 was added to a
352 final concentration of 4 ng/mL and incubated at room temperature for 5 minutes. Cells
353 were then fixed with 2% paraformaldehyde for one hour at room temperature, and
354 washed and resuspended in PBS+Tween80 for imaging.
355
356 *Microscopy. Mab* cells were resuspended as described for plating of planktonic and
357 biofilm cells, then fixed with 4% paraformaldehyde in PBS at room temperature for 2
358 hours. Cells were immobilized on agarose pads and imaged using a Nikon Ti-2
359 widefield epifluorescence microscope with a Photometrics Prime 95B camera and a
360 Plan Apo 100X, 1.45 NA objective. Green fluorescent images were taken using a filter
361 cube with a 470/40 nm excitation filter and a 525/50nm emission filter. Red fluorescent
362 images were taken using a filter cube with a 560/40nm excitation filter and a 630/70
363 emission filter. Images were captured using NIS Elements software and analyzed using
364 FIJI and MicrobeJ (45).
365
366 **References**
367

1. **World Health Organization**. 2016. Global Tuberculosis Report.

2. **Brode SK**, **Daley CL**, **Marras TK**. 2014. The epidemiologic relationship between tuberculosis and non-tuberculous mycobacterial disease: a systematic review. int j tuberc lung dis **18**:1370–1377.

3. **Stout JE**, **Koh W-J**, **Yew WW**. 2016. Update on pulmonary disease due to non-tuberculous mycobacteria. International Journal of Infectious Diseases **45**:123–134.

4. **Cystic Fibrosis Foundation**. 2017. 2016 Patient Registry Annual Data Report 1–94.

5. **Bar-On O**, **Mussaffi H**, **Mei-Zahav M**, **Prais D**, **Steuer G**, **Stafler P**, **Hananya S**, **Blau H**. 2015. Increasing nontuberculous mycobacteria infection in cystic fibrosis. Journal of Cystic Fibrosis **14**:53–62.

6. **Esther CR Jr**, **Esserman DA**, **Gilligan P**, **Kerr A**, **Noone PG**. 2010. Chronic Mycobacterium abscessus infection and lung function decline in cystic fibrosis. Journal of Cystic Fibrosis **9**:117–123.

7. **Bryant JM**, **Grogono DM**, **Rodriguez-Rincon D**, **Everall I**, **Brown KP**, **Moreno P**, **Verma D**, **Hill E**, **Drijkoningen J**, **Gilligan P**, **Esther CR**, **Noone PG**, **Giddings O**, **Bell SC**, **Thomson R**, **Wainwright CE**, **Coulter C**, **Pandey S**, **Wood ME**, **Stockwell RE**, **Ramsay KA**, **Sherrard LJ**, **Kidd TJ**, **Jabbour N**, **Johnson GR**, **Knibbs LD**, **Morawska L**, **Sly PD**, **Jones A**, **Bilton D**, **Laurenson I**, **Ruddy M**, **Bourke S**, **Bowler ICJW**, **Chapman SJ**, **Clayton A**, **Cullen M**, **Dempsey O**, **Denton M**, **Desai M**, **Drew RJ**, **Edenborough F**, **Evans J**, **Folb J**, **Daniels T**, **Humphrey H**, **Isalska B**, **Jensen-Fangel S**, **Jönsson B**, **Jones AM**, **Katzenstein TL**, **Lillebaek T**, **MacGregor G**, **Mayell S**, **Millar M**, **Modha D**, **Nash EF**, **O'Brien C**, **O'Brien D**, **Ohri C**, **Pao CS**, **Peckham D**, **Perrin F**, **Perry A**, **Pressler T**, **Prtak L**, **Qvist T**, **Robb A**, **Rodgers H**, **Schaffer K**, **Shafi N**, **van Ingen J**, **Walshaw M**, **Watson D**, **West N**, **Whitehouse J**, **Haworth CS**, **Harris SR**, **Ordway D**, **Parkhill J**, **Floto RA**. 2016. Emergence and spread of a human-transmissible multidrug-resistant nontuberculous mycobacterium. Science **354**:751–757.

8. **DaCosta A**, **Jordan CL**, **Giddings O**, **Lin F-C**, **Gilligan P**, **Esther CR Jr**. 2017. Outcomes associated with antibiotic regimens for treatment of Mycobacterium abscessus in cystic fibrosis patients. Journal of Cystic Fibrosis 1–5.

9. **Rominski A**, **Selchow P**, **Becker K**, **Brülle JK**, **Dal Molin M**, **Sander P**. 2017. Elucidation of Mycobacterium abscessus aminoglycoside and capreomycin resistance by targeted deletion of three putative resistance genes. Journal of Antimicrobial Chemotherapy 1–10.

407 10. **Rominski A**, **Roditscheff A**, **Selchow P**, **Böttger EC**, **Sander P**. 2017.
408 Intrinsic rifamycin resistance of Mycobacterium abscessusis mediated by
409 ADP-ribosyltransferase MAB_0591. Journal of Antimicrobial Chemotherapy
410 **72**:376–384.

411 11. **Hurst-Hess K**, **Rudra P**, **Ghosh P**. 2017. Mycobacterium abscessus WhiB7
412 Regulates a Species-Specific Repertoire of Genes To Confer Extreme
413 Antibiotic Resistance. Antimicrobial Agents and Chemotherapy **61**:e01347–
414 17–11.

415 12. **Greendyke R**, **Byrd TF**. 2008. Differential Antibiotic Susceptibility of
416 Mycobacterium abscessus Variants in Biofilms and Macrophages Compared
417 to That of Planktonic Bacteria. Antimicrobial Agents and Chemotherapy
418 **52**:2019–2026.

419 13. **Qvist T**, **Eickhardt S**, **Kragh K**, **Andersen C**, **Iverson M**, **Høiby N**,
420 **Bjarnsholt T**. 2015. Chronic pulmonary disease with Mycobacterium
421 abscessus complex is a biofilm infection. Eur Respiratory Soc **46**:1823–
422 1826.

423 14. **Flemming HC**, **Neu TR**, **Wozniak DJ**. 2007. The EPS Matrix: The "House of
424 Biofilm Cells." J Bacteriol **189**:7945–7947.

425 15. **Recht J**, **Martínez A**, **Torello S**, **Kolter R**. 2000. Genetic analysis of sliding
426 motility in Mycobacterium smegmatis. J Bacteriol **182**:4348–4351.

427 16. **Ojha A**, **Anand M**, **Bhatt A**, **Kremer L**, **Jacobs WR Jr.**, **Hatfull GF**. 2005.
428 GroEL1: A Dedicated Chaperone Involved in Mycolic Acid Biosynthesis
429 during Biofilm Formation in Mycobacteria. Cell **123**:861–873.

430 17. **Ojha AK**, **Baughn AD**, **Sambandan D**, **Hsu T**, **Trivelli X**, **Guérardel Y**,
431 **Alahari A**, **Kremer L**, **Jacobs WR Jr.**, **Hatfull GF**. 2008. Growth of
432 Mycobacterium tuberculosisbiofilms containing free mycolic acids and
433 harbouring drug-tolerant bacteria. Mol Microbiol **69**:164–174.

434 18. **Stewart P**. 2015. Antimicrobial tolerance in biofilms. Microbiology Spectrum
435 **doi:10.1128/microbiolspec.MB-0010-2014**.

436 19. **Clary G**, **Sasindran SJ**, **Nesbitt N**, **Mason L**, **Cole S**, **Azad A**, **McCoy K**,
437 **Schlesinger LS**, **Hall-Stoodley L**. 2018. Mycobacterium abscessusSmooth
438 and Rough Morphotypes Form Antimicrobial-Tolerant Biofilm Phenotypes
439 but Are Killed by Acetic Acid. Antimicrobial Agents and Chemotherapy
440 **62**:e01782–17–17.

441 20. **Gutiérrez AV**, **Viljoen A**, **Ghigo E**, **Herrmann J-L**, **Kremer L**. 2018.
442 Glycopeptidolipids, a Double-Edged Sword of the Mycobacterium abscessus
443 Complex. Front Microbiol **9**:E943–8.

21. **Davidson LB**, **Nessar R**, **Kempaiah P**, **Perkins DJ**, **Byrd TF**. 2011. Mycobacterium abscessus Glycopeptidolipid Prevents Respiratory Epithelial TLR2 Signaling as Measured by HβD2 Gene Expression and IL-8 Release. PLoS ONE **6**:e29148–8.

22. **Hunter RL**, **Olsen MR**, **Jagannath C**, **Actor JK**. 2006. Multiple roles of cord factor in the pathogenesis of primary, secondary, and cavitary tuberculosis, including a revised description of the pathology of secondary disease. Ann Clin Lab Sci **36**:371–386.

23. **Byrd TF**, **Lyons CR**. 1999. Preliminary characterization of a Mycobacterium abscessus mutant in human and murine models of infection. Infection and immunity **67**:4700–4707.

24. **Howard ST**. 2006. Spontaneous reversion of Mycobacterium abscessus from a smooth to a rough morphotype is associated with reduced expression of glycopeptidolipid and reacquisition of an invasive phenotype. Microbiology (Reading, Engl) **152**:1581–1590.

25. **Kreutzfeldt KM**, **McAdam PR**, **Claxton P**, **Holmes A**, **Seagar AL**, **Laurenson IF**, **Fitzgerald JR**. 2013. Molecular Longitudinal Tracking of Mycobacterium abscessus spp. during Chronic Infection of the Human Lung. PLoS ONE **8**:e63237–9.

26. **Park IK**, **Hsu AP**, **Tettelin H**, **Shallom SJ**, **Drake SK**, **Ding L**, **Wu U-I**, **Adamo N**, **Prevots DR**, **Olivier KN**, **Holland SM**, **Sampaio EP**, **Zelazny AM**. 2015. Clonal Diversification and Changes in Lipid Traits and Colony Morphology in Mycobacterium abscessus Clinical Isolates. J Clin Microbiol, 6 ed. **53**:3438–3447.

27. **Palmer KL**, **Aye LM**, **Whiteley M**. 2007. Nutritional Cues Control Pseudomonas aeruginosa Multicellular Behavior in Cystic Fibrosis Sputum. J Bacteriol **189**:8079–8087.

28. **Kuru E**, **Hughes HV**, **Brown PJ**, **Hall E**, **Tekkam S**, **Cava F**, **de Pedro MA**, **Brun YV**, **VanNieuwenhze MS**. 2012. In Situ Probing of Newly Synthesized Peptidoglycan in Live Bacteria with Fluorescent D-Amino Acids. Angew Chem Int Ed **51**:12519–12523.

29. **Fishov I**, **Woldringh CL**. 1999. Visualization of membrane domains in Escherichia coli. Mol Microbiol **32**:1166–1172.

30. **Aldridge BB**, **Fernandez-Suarez M**, **Heller D**, **Ambravaneswaran V**, **Irimia D**, **Toner M**, **Fortune SM**. 2012. Asymmetry and Aging of Mycobacterial Cells Lead to Variable Growth and Antibiotic Susceptibility. Science **335**:100–104.

481 31. **Burbaud S**, **Laval F**, **Lemassu A**, **Daffé M**, **Guilhot C**, **Chalut C**. 2016.
482 Trehalose Polyphleates Are Produced by a Glycolipid Biosynthetic Pathway
483 Conserved across Phylogenetically Distant Mycobacteria. Cell Chemical
484 Biology **23**:278–289.

485 32. **Wayne LG**, **Hayes LG**. 1996. An in vitro model for sequential study of
486 shiftdown of Mycobacterium tuberculosis through two stages of
487 nonreplicating persistence. Infection and immunity **64**:2062–2069.

488 33. **Schaechter M**, **Microbiology OM**, **1958**. 1958. Dependency on Medium
489 and Temperature of Cell Size and Chemical Composition during Balanced
490 Growth of Salmonella typhimurium. J Gen Microbiol **19**:592–606.

491 34. **Ojha AK**, **Varma S**, **Chatterji D**, **(null)**. 2002. Synthesis of an unusual polar
492 glycopeptidolipid in glucose-limited culture of Mycobacterium smegmatis.
493 Microbiology **148**:3039–3048.

494 35. **Blair JMA**, **Richmond GE**, **Bailey AM**, **Ivens A**, **Piddock LJV**. 2013.
495 Choice of Bacterial Growth Medium Alters the Transcriptome and Phenotype
496 of Salmonella enterica Serovar Typhimurium. PLoS ONE **8**:e63912–8.

497 36. **Kostakioti M**, **Hadjifrangiskou M**, **Hultgren SJ**. 2013. Bacterial Biofilms:
498 Development, Dispersal, and Therapeutic Strategies in the Dawn of the
499 Postantibiotic Era. Cold Spring Harb Perspect Med **3**:a010306–a010306.

500 37. **Landry RM**, **An D**, **Hupp JT**, **Singh PK**, **Parsek MR**. 2006. Mucin-
501 Pseudomonas aeruginosa interactions promote biofilm formation and
502 antibiotic resistance. Mol Microbiol **59**:142–151.

503 38. **Jackson LMD**, **Kroukamp O**, **Wolfaardt GM**. 2015. Effect of carbon on
504 whole-biofilm metabolic response to high doses of streptomycin. Front
505 Microbiol **6**:1114–14.

506 39. **Serra DO**, **Richter AM**, **Klauck G**, **Mika F**, **Hengge R**. 2013. Microanatomy
507 at Cellular Resolution and Spatial Order of Physiological Differentiation in a
508 Bacterial Biofilm. mBio **4**:e00103–13–e00103–13.

509 40. **Besharova O**, **Suchanek VM**, **Hartmann R**, **Drescher K**, **Sourjik V**. 2016.
510 Diversification of Gene Expression during Formation of Static Submerged
511 Biofilms by Escherichia coli. Front Microbiol **7**:717–17.

512 41. **Williamson KS**, **Richards LA**, **Perez-Osorio AC**, **Pitts B**, **McInnerney K**,
513 **Stewart PS**, **Franklin MJ**. 2012. Heterogeneity in Pseudomonas aeruginosa
514 Biofilms Includes Expression of Ribosome Hibernation Factors in the
515 Antibiotic-Tolerant Subpopulation and Hypoxia-Induced Stress Response in
516 the Metabolically Active Population. J Bacteriol **194**:2062–2073.

517 42. **Xie Z**, **Siddiqi N**, **Rubin EJ**. 2005. Differential Antibiotic Susceptibilities of
518 Starved Mycobacterium tuberculosis Isolates. Antimicrobial Agents and
519 Chemotherapy **49**:4778–4780.

520 43. **Hartmans S**, **De Bont JAM**. 1992. The genus *Mycobacterium*— nonmedical

521 , 2nd ed. Springer-Verlag New York Inc., New York, NY.

522 44. **Sriramulu DD**. 2005. Microcolony formation: a novel biofilm model of
523 Pseudomonas aeruginosa for the cystic fibrosis lung. Journal of Medical
524 Microbiology **54**:667–676.

525 45. **Ducret A**, **Quardokus EM**, **Brun YV**. 2016. MicrobeJ, a tool for high
526 throughput bacterial cell detection and quantitative analysis. Nature
527 Microbiology **1**:1–7.

528

529 **Figures and Figure Legends**

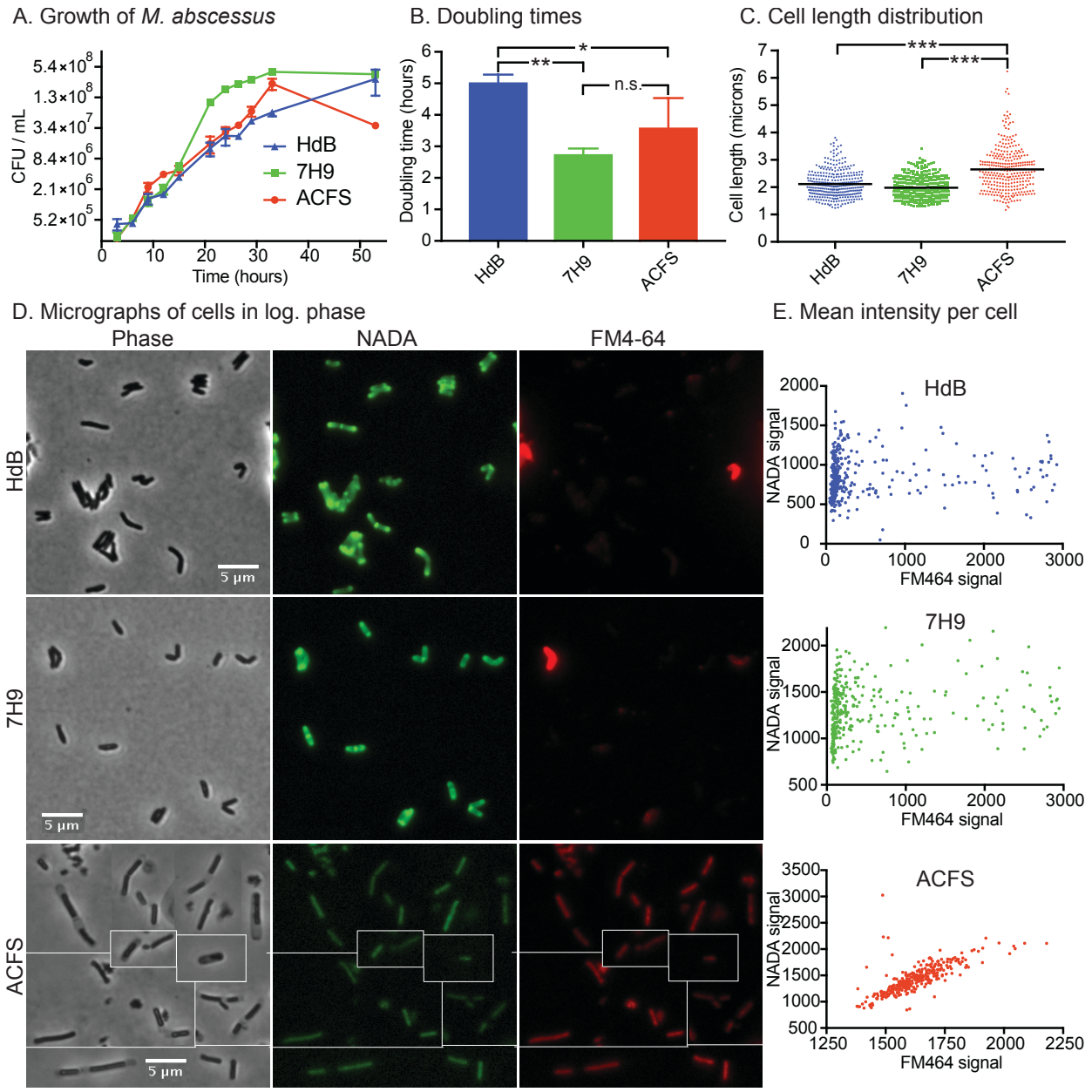

530

531

532

533 **Figure 1. The physiology of *Mab* planktonic cells varies according to media type.**

534 A) Colony forming units over time in the three growth media on a 2-log scale. B)

535 Maximum doubling times during log. phase growth, calculated from data in (A). P values

536 calculated by one-way ANOVA with Tukey correction. Hdb vs. 7H9, P=0.0059; Hdb vs.

537 ACFS, P=0.0459. C) Quantification of cell lengths of *Mab* cells in log. phase, in the
538 three media types. At least 300 cells from two biological replicates were imaged by
539 phase microscopy and cell lengths were calculated using MicrobeJ. ACFS vs. HdB,
540 P<0.0001; ACFS vs. 7H9, P<0.0001. D) Micrographs of log. phase cells stained with the
541 fluorescent D-amino acid NADA and the membrane stain FM4-64. E) Quantification of
542 the average fluorescent intensity for at least 300 cells from two biological replicates,
543 stained with NADA and FM4-64, as in (D).
544
545
546
547
548
549

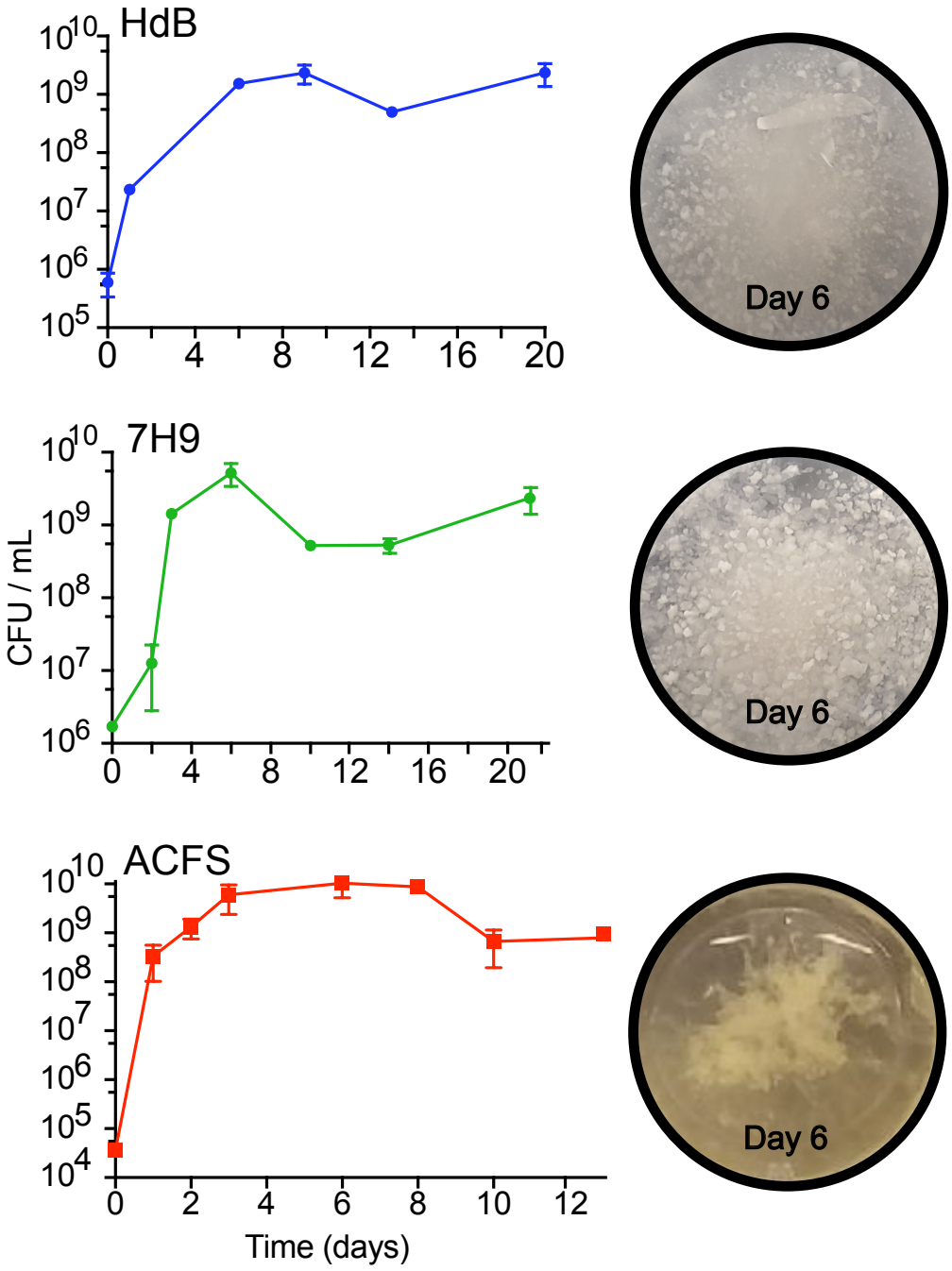

550

551 **Figure 2. The development and macroscopic structure of *Mab* biofilms in different**

552 **media.** Colony forming units for biofilm-associated cells in standing culture over time.

553 Images of corresponding wells taken at 6 days.

A. Micrographs of Live/Dead reporter in ACFS

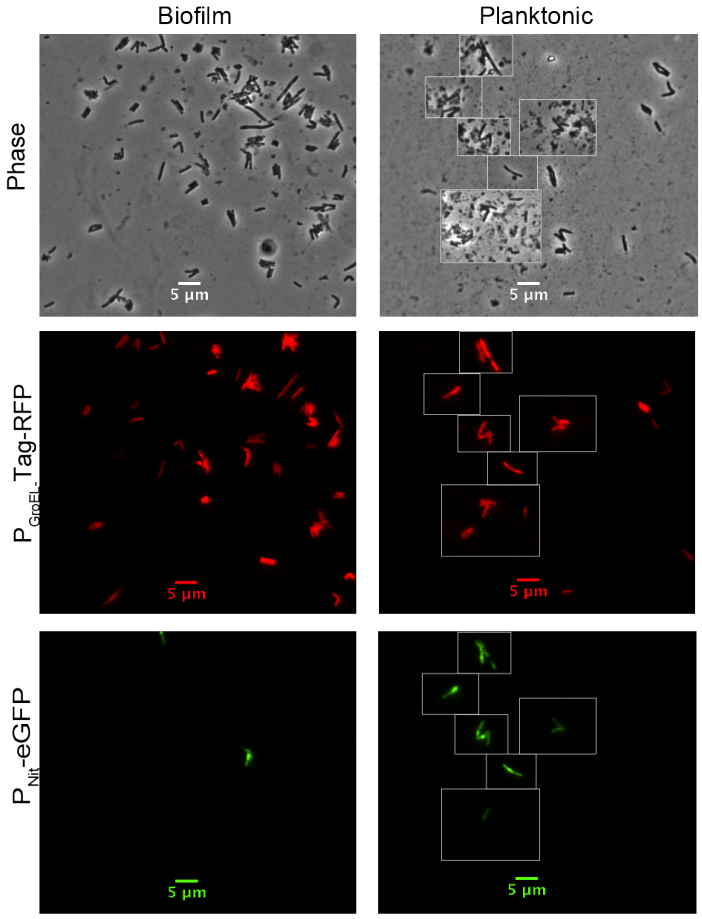

B. Percent induced in ACFS, 7H9 and HdB

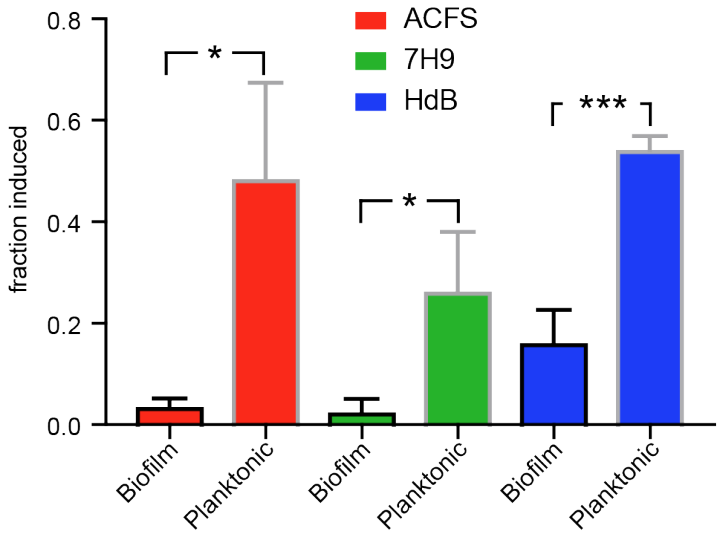

554

555 **Figure 3. Cells in *Mab* biofilms are less responsive to a transcriptional inducer.**
556 (A) Micrographs of *Mab* cells carrying the pDE43-MEK-Nit-live/dead vector from biofilms
557 grown for 6 days in ACFS, then induced with 10^{-6} isovaleronitrile for one day before
558 fixation and imaging. Living cells that retain the vector show constitutive Tag-RFP
559 signal, inducible cells also show eGFP signal. (B) Percentage of cells with average Tag-
560 RFP signal intensities above 400 that also have average eGFP signal intensities above
561 100 in each condition. At least 100 cells each from three independent biological
562 replicates were quantified for each condition. P-value of biofilm vs. planktonic for ACFS,
563 7H9 and HdB medias are 0.0152, 0.0271 and 0.0007, respectively. P-values were
564 calculated using an unpaired t-test.
565

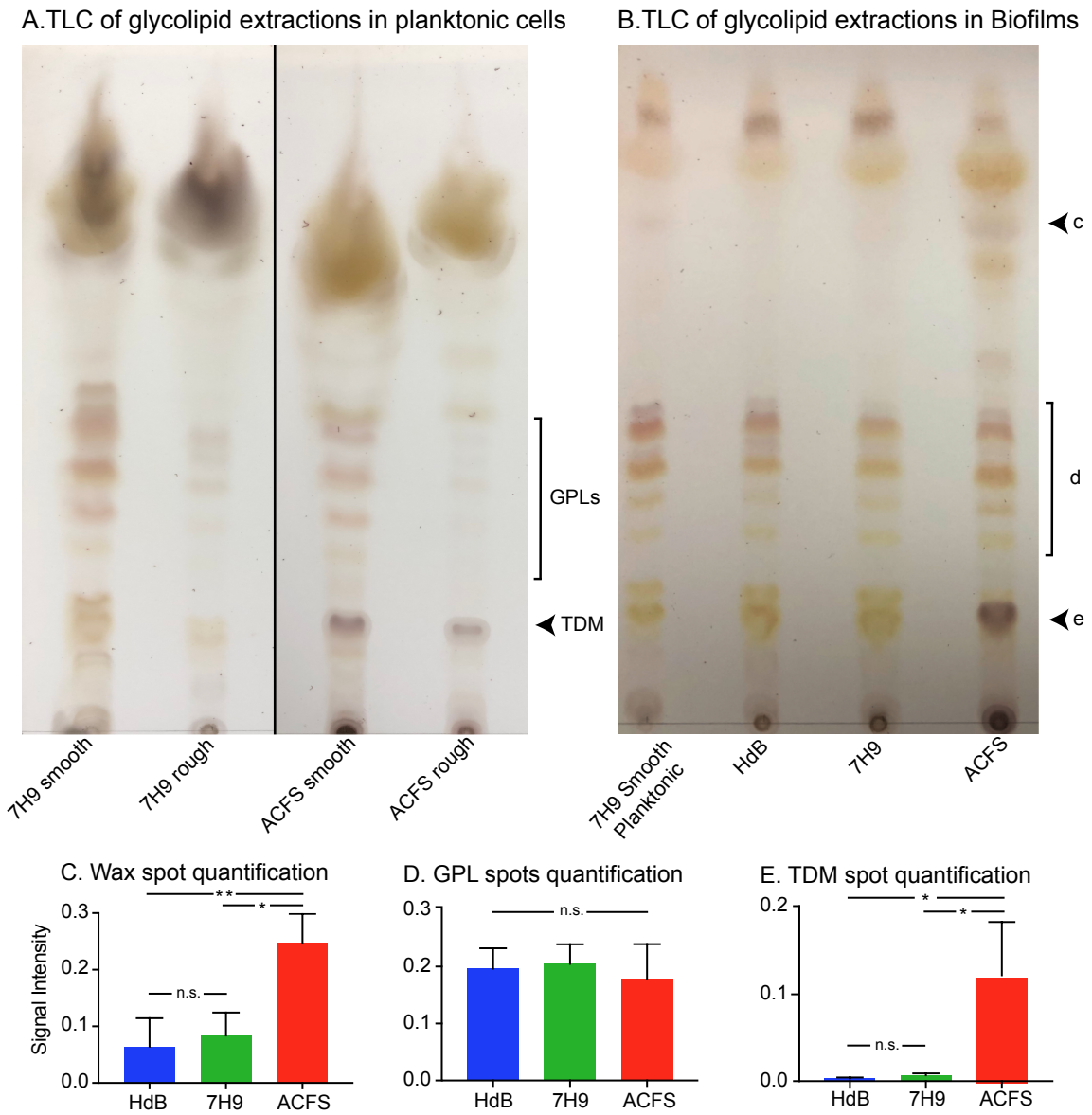

Figure 4. Glycolipid profiles are affected by media condition. (A) Thin Layer Chromatography (TLC) of glycolipid extractions from planktonic cultures of rough and smooth *Mab* strains grown in 7H9 and ACFS. GPLs = glycopeptidolipids, TDM= trehalose dimycolate. (B) Representative TLC of glycolipid extracts from mature biofilms of smooth *Mab* in Hdb, 7H9 and ACFS. Extraction from planktonic cells grown in 7H9 + Tween80 was used as a control sample. Black arrows indicate lipid species prominent

574 in ACFS: c - unknown wax; d – GPLs; e - TDM. (C, D, E) Quantification of the signal
575 intensity for each spot in (B) by means of spot densitometry. Values shown are the
576 mean of three biological replicate experiments with error bars representing the standard
577 deviation. (C) Wax, P-values between ACFS vs. Hdb and ACFS vs. 7H9 were 0.0079
578 and 0.0134, respectively. (D) GPLs, no significant differences. (E) TDM, P-values
579 between ACFS vs. Hdb and ACFS vs. 7H9 were 0.0149 and 0.0171, respectively. P-
580 values were calculated using one-way ANOVA with Tukey correction for multiple
581 comparisons. Signal intensities for (D) were quantified by using the red channel only of
582 the TLC images, to eliminate the signal from the yellow spots in the same area.

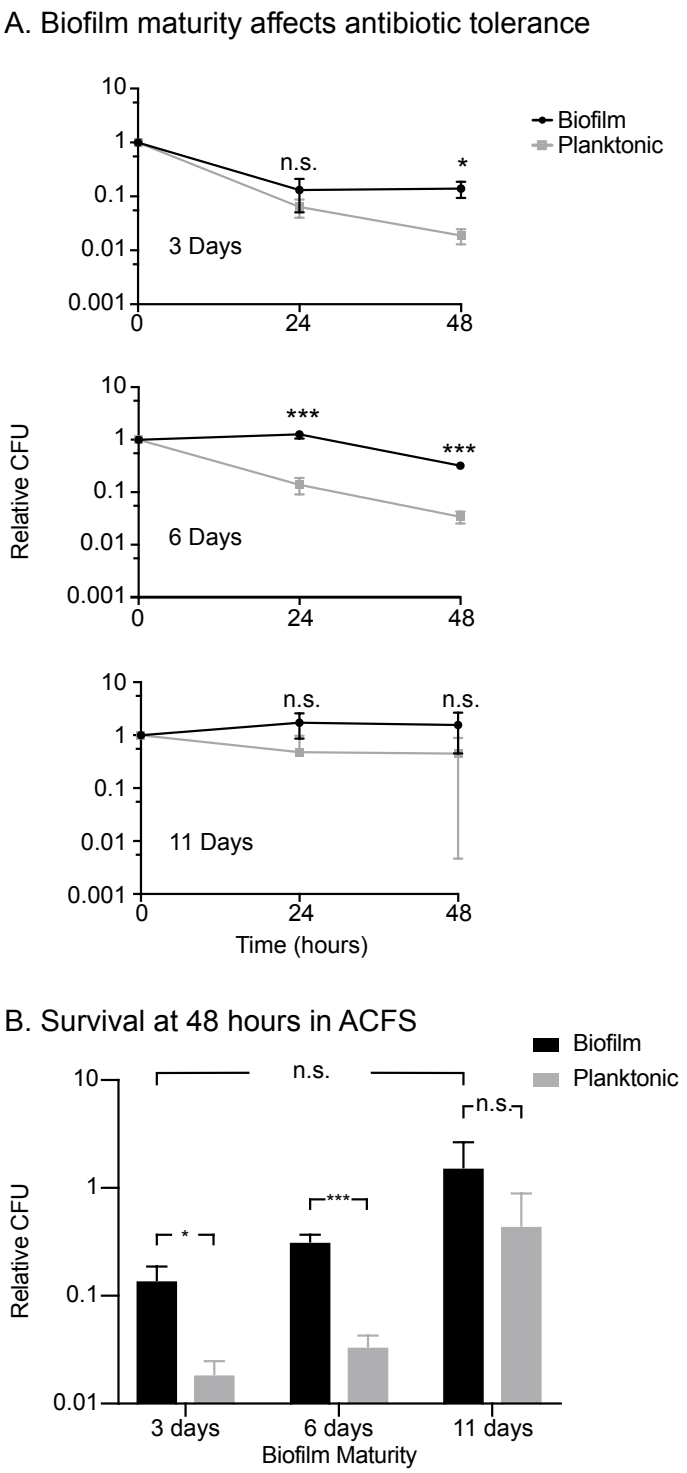

583

584 **Figure 5. Antibiotic tolerance increases as ACFS biofilms mature.** (A) Relative

585 CFUs (CFU at each time point divided by the CFU value before treatment, *i.e.*, t=0) from

586 biofilms and planktonic cells from the same wells, grown for 3, 6 and 11 days in ACFS.

587 Cultures were treated with clarithromycin (20 μg/mL) and imipenem (15 μg/mL) for 48
588 hours, and CFUs were measured at 0, 24 and 48 hours. (B) Survival from 48-hour CFU
589 time points (triplicate wells). P-values between biofilm and planktonic cells are 0.01099,
590 0.0006, 0.1815, for 3, 6, and 11 days respectively. P-value for biofilms between 3 and
591 11 days is 0.09046. P-values were calculated using the student's t-test.
592

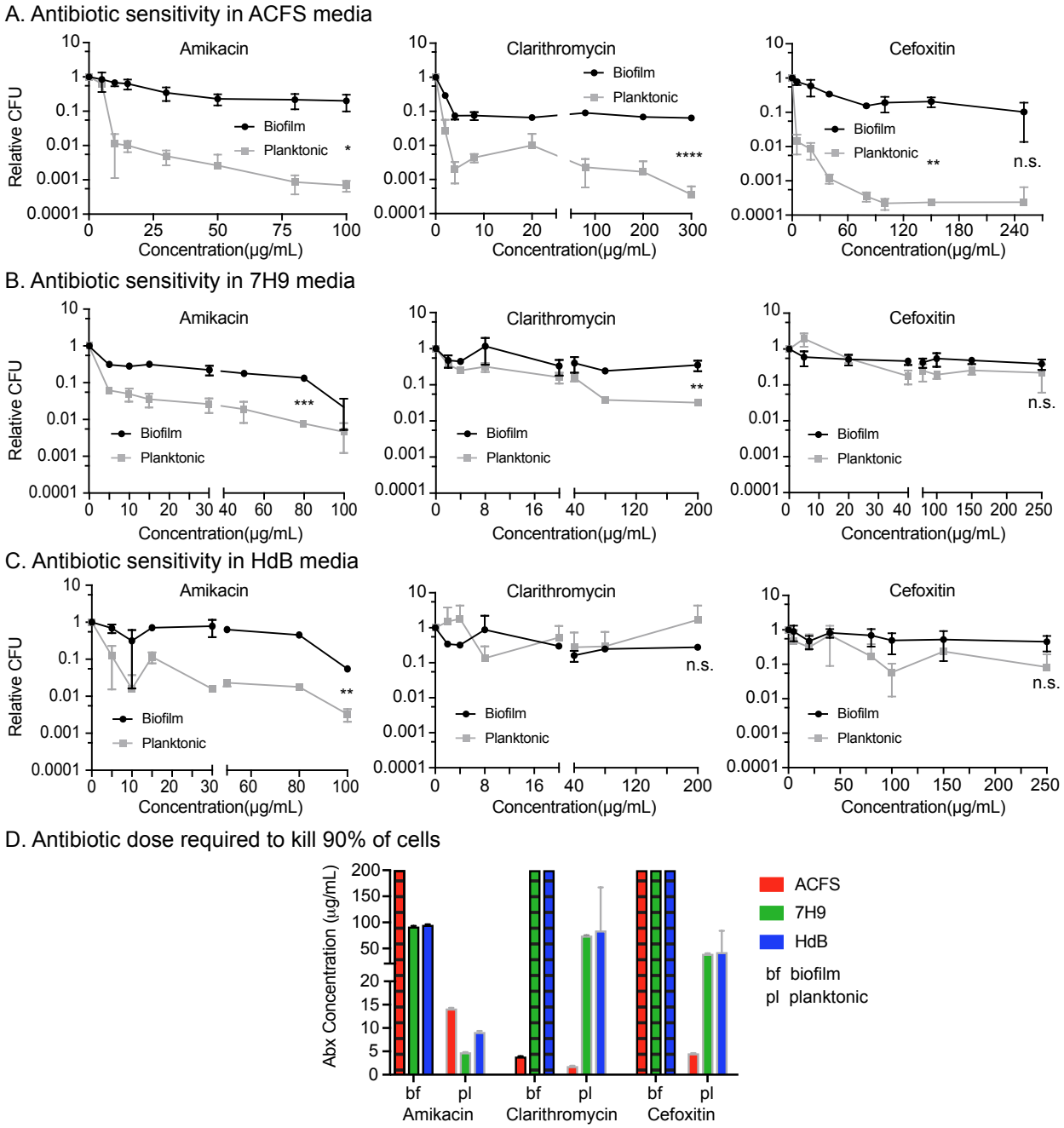

Figure 6. Antibiotic sensitivity varies by antibiotic and media type. (A, B, C) Relative CFUs of 6-day old biofilms and planktonic cells from the same wells after 48 hours of treatment with a range of antibiotic concentrations in 3 medias. Asterisks represent significance as measured by the student's t-test; * = P ≤ 0.05; ** = P ≤ 0.01; *** = P ≤ 0.001; n.s. = P > 0.05. (D) LD90 (dose required to kill 90% of the cells)

599 analysis of the data from A, B and C. Bars with hatched lines indicate that we were
600 unable to observe killing of 90% of the population at any concentration used, so the
601 LD90 is above 200 μg/mL. The LD90 was calculated for each replicate and the bars
602 indicate mean and with standard deviation.
603